ChemComm

COMMUNICATION

View Article Online
View Journal | View Issue

Cite this: *Chem. Commun.*, 2019, **55**, 10456

Received 16th July 2019,
Accepted 7th August 2019

DOI: 10.1039/c9cc05346h

rsc.li/chemcomm

Bio-orthogonal chemistry-based method for fluorescent labelling of ribosomal RNA in live mammalian cells†

K. Wu,[a] M. He,[a] I. Khan,[a] P. N. Asare Okai,[b] Q. Lin,[a] G. Fuchs[a] and M. Royzen*[a]

A bio-orthogonal chemistry-based approach for fluorescent labelling of ribosomal RNA is described. It involves an adenosine analogue modified with *trans*-cyclooctene and masked 5′-phosphate group using aryl phosphoramidate. The incorporation into rRNA has been confirmed using agarose gel electrophoresis, as well as a highly sensitive UHPLC-MS/MS method. Fluorescent labelling of rRNA has been achieved in live HeLa cells *via* an inverse electron demand Diels–Alder reaction with a tetrazine conjugated to an Oregon Green fluorophore. This communication describes the stepwise approach that led to the development and characterization of the probe. The results demonstrate a new strategy towards development of future fluorescent probes to investigate the biochemistry of nucleic acids.

There is a strong interest in developing imaging tools to understand the structural and functional diversity of RNA.[1] One striking example was reported by Singer and co-workers who developed an imaging technique to visualize neuronal β-actin messenger RNA. The reported technique allowed an investigation of molecular mechanisms underlying memory formation in a mouse brain. Discoveries like these foster enthusiasm to tackle many yet unanswered fundamental questions about biochemistry of RNA.[2]

One approach is to tag biomolecules with a bio-orthogonal reporter group that minimally perturbs the native structure and remains chemically inert to the functional groups found inside the cell. Once the biomolecule is metabolized by the cell, imaging is enabled upon reaction with the fluorescently-labelled bio-orthogonal partner, as shown in Scheme 1A. During the past decade, this strategy has been extensively explored for labelling and visualizing a wide range of biomolecules. For example, strain-promoted Cu-free click chemistry has been shown to be highly efficient to visualize glycans.[3] The bio-orthogonal inverse electron demand Diels–Alder (IEDDA) chemistry has been used for imaging of cellular membranes.[4] IEDDA chemistry has also been explored for site-specific modification of proteins, followed by fluorescent imaging.[5]

Conservative modifications of canonical nucleobases have been shown to be tolerated by biosynthetic enzymes, enabling the metabolic incorporation of bio-orthogonal groups into oligonucleotides. The classical example is 5-bromouridine (**BrU**), shown in Scheme 1B. **BrU** is taken up by cells and incorporated into cellular RNAs by means of the ribonucleoside salvage pathway. The metabolized **BrU** can subsequently be detected by immunostaining.[6] Copper-catalyzed azide–alkyne 1,3-dipolar cycloaddition (CuAAC) chemistry fostered development of a series of alkyne-modified nucleosides, **EU**, **EC** and **EA**, shown in Scheme 1B.[7] Their incorporation into cellular RNAs is thought to be analogous to **BrU**, while fluorescent labelling has been achieved by 'click' reaction with fluorescent azides. In recent years, the two uridine analogues, **TU** and **VU**, have been reported. The former was labelled using 4-bromomethyl-7-propargyloxycoumarin, while the latter *via* [4+2] cycloaddition with phenyl triazolinedione.[8]

The IEDDA reaction between TCO and tetrazine (Tz) offers an attractive opportunity for fluorescent labelling of nascent cellular RNA. This chemistry has been shown to be compatible with RNA.[9] A number of literature reports described different applications of IEDDA chemistry for fluorescent labelling of synthetic RNA strands in solution and in live cells.[10] This is one of the fastest known bio-orthogonal reactions thus facilitating the development of quick protocols for fluorescent labelling of cellular RNA.[11] Unlike CuAAC chemistry, the reaction between TCO and Tz does not require copper catalysis. Thus, RNA labelling can be done in live cells. Until recently however TCO and Tz groups have been considered too large to be masked on the surface of nucleosides. The present communication aims to disprove this notion by describing a TCO-containing nucleoside capable of incorporating into *de novo* synthesized ribosomal RNA inside of live mammalian cells. Its incorporation was established using fluorescence microscopy, gel electrophoresis and a UHPLC-MS/MS technique.

[a] *University at Albany, SUNY, Department of Chemistry, 1400 Washington Ave., Albany, NY 12222, USA. E-mail: mroyzen@albany.edu*
[b] *University of Delaware, Department of Chemistry and Biochemistry, Brown Labs, Newark, DE 19716, USA*

† Electronic supplementary information (ESI) available. See DOI: 10.1039/c9cc05346h

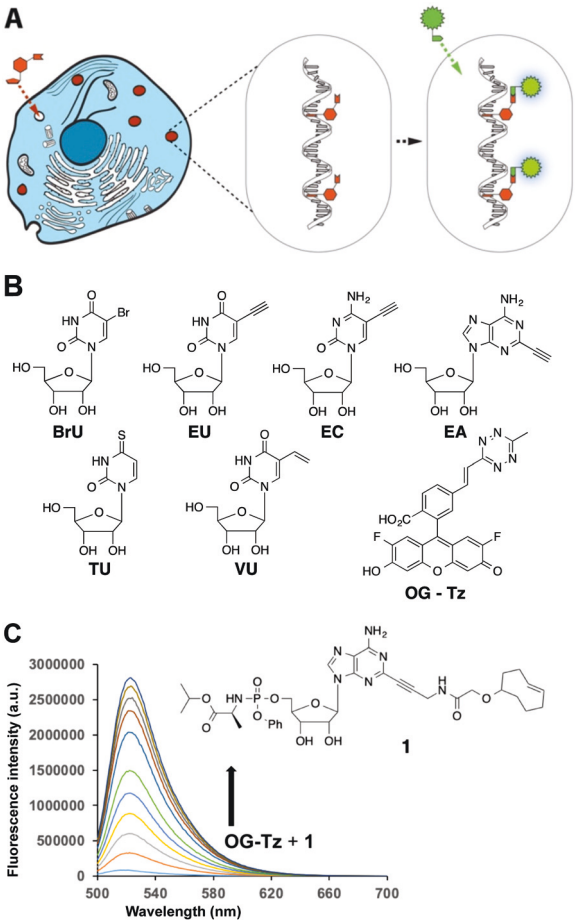

Scheme 1 (A) Bio-orthogonal approach for fluorescent labeling of cellular RNA. (B) Reported nucleoside analogues that incorporate into cellular RNA. Oregon Green dye modified with 1,2,4,5-tetrazine, **OG-Tz**, that allows fluorescent labeling of RNA. (C) Enhancement of Oregon Green fluorescence when **OG-Tz** (10 μM) is titrated with **1** (1 μM).

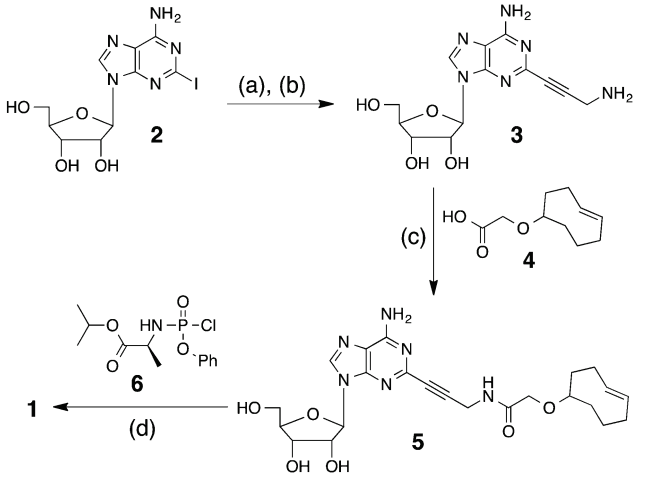

Scheme 2 Synthesis of compound **1**: (a) TFA–propargyl amine, $Pd(PPh_3)_4$, CuI, DIPEA, DMF; (b) NH_4OH, H_2O; (c) HATU, DIPEA, DMF; (d) *N*-methyl imidazole, THF.

We were inspired by the report by Jaffrey and co-workers describing incorporation of **EA** into cellular RNA during transcription and poly-adenylation.[7c] Our goal was to investigate if a larger modification at the 2-position of adenosine would be tolerated by the cellular metabolic machinery. We designed compound **1**, shown in Scheme 1C. In addition to the bio-orthogonal handle, it contains a masked 5′-monophosphate in a form of aryl phosphoramidate. It's been well established that the key step towards incorporation of modified nucleosides into cellular RNAs is recognition by their respective kinases that install phosphates at the 5′-hydroxy group.[12] To circumvent this challenge, a 5′-monophosphate group can be pre-installed in a form of aryl phosphoramidate.[13] Enzymatic hydrolysis of aryl phosphoramidates inside the cell leads to its conversion to 5′-monophosphate group.

Compound **1** was synthesized in 4 steps, described in Scheme 2. The synthesis commenced with the commercially available 2-iodoadenosine. The TFA-protected propargyl amine was installed using Sonogashira coupling conditions. Removal of the protecting group using aqueous ammonia afforded the amine **3**. Coupling of the previously reported carboxylic acid **4** produced compound **5**. The target compound **1** was achieved upon addition of the aryl phosphoramidate group **6**.

To detect incorporation of **1** into cellular RNAs, we followed a highly sensitive UHPLC-MS/MS approach recently described by Agris and co-workers and illustrated in Fig. 1A.[14] HeLa cells were treated with the adenosine analogue for 24 h, followed by isolation of the total cellular RNA (RNA Bee kit, AMS Biotechnology). The total cellular RNA was hydrolyzed to the composite mononucleosides *via* a two-step enzymatic hydrolysis with nuclease P1, followed by bacterial alkaline phosphatase. The sensitivity of the aforementioned method allows quantification of RNA modification levels down to attomolar concentrations.

The UHPLC-MS/MS analysis verified incorporation of **1** into cellular RNA. After the enzymatic hydrolysis of cellular RNA, described in Fig. 1A, we were able to detect the unnatural nucleoside **5**, in addition to the native A, U, C and G. Detections of fragments **X** and **Y**, shown in Fig. 1B was first established with a standard sample of **5**. The UHPLC-MS/MS spectra of **5** is shown in Fig. 1C and D. We observed 2 peaks on each spectrum, as **5** was synthesized as a diastereomeric mixture. We were gratified to observe the same two peaks (Fig. 1E and F) from the total cellular RNA extract. To further pinpoint where **1** gets incorporated, we purified total cellular mRNAs using magnetic beads modified with poly-T DNA strands (New England Biolabs). We were anticipating enriched incorporation of the adenosine analogue into poly-A tails of mRNA. To our surprise, the UHPLC MS/MS analysis failed to produce any detectable signal corresponding to **5** (Fig. 1G and H), thus suggesting that **1** does not incorporate into cellular mRNAs. We subsequently followed an established procedure to purify ribosomal RNA from HeLa cells.[15] The procedure entailed ribosome pelleting through a 30% sucrose cushion and subsequent extraction of rRNA using TRIzol. After the aforementioned enzymatic hydrolysis of the purified rRNA, we obtained the UHPLC MS/MS spectra shown in Fig. 1I and J. A highly enriched MS/MS signal corresponding to the adenosine analogue has been observed

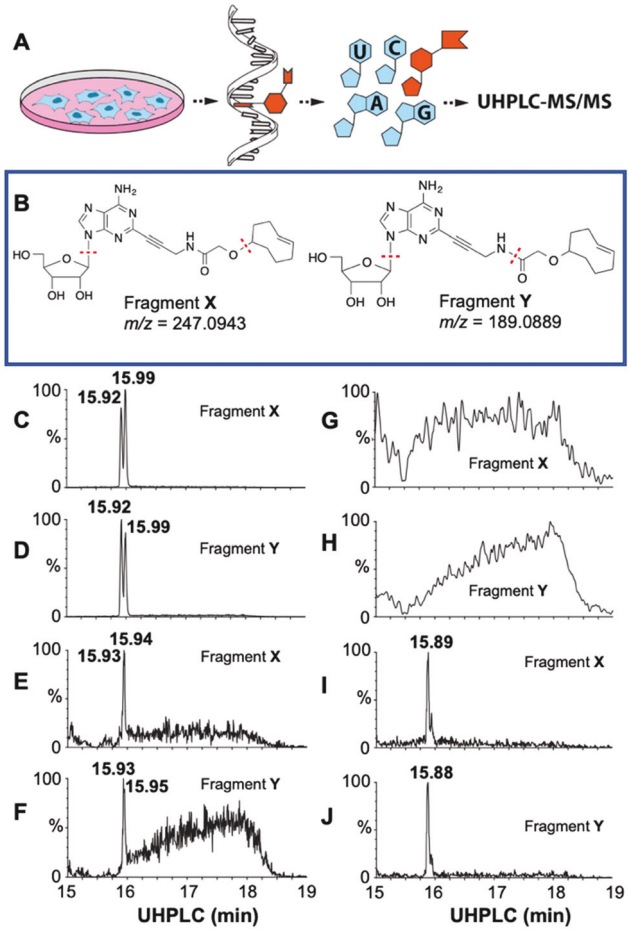

Fig. 1 (A) Schematic representation of sample preparation for UHPLC MS/MS analysis. (B) Fragmentation of the adenosine analogue observed by the MS/MS analysis. UHPLC MS/MS spectra: (C) detection of the fragment **X** from the standard sample of **5**; (D) detection of the fragment **Y** from the standard sample of **5**; (E) detection of the fragment **X** from the total RNA extract from HeLa cells; (F) detection of the fragment **Y** from the total RNA extract from HeLa cells; (G) detection of the fragment **X** from total mRNA purified from HeLa cells; (H) detection of the fragment **Y** from total mRNA purified from HeLa cells; (I) detection of the fragment **X** from the ribosomal RNA purified from HeLa cells; (J) detection of the fragment **Y** from the total RNA purified from HeLa cells.

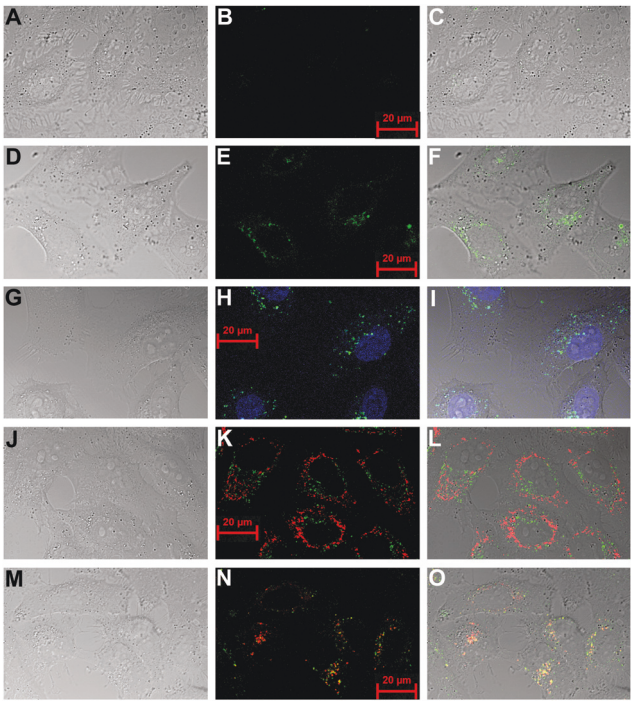

Fig. 2 Fluorescence imaging of ribosomal RNA in HeLa cells. First row: (A) brightfield, (B) green channel, (C) overlay of brightfield and green channels of cells treated with DMSO and subsequently **OG-Tz** (negative control); second row: (D) brightfield, (E) green channel, (F) overlay of brightfield and green channels of cells treated with **1** and subsequently **OG-Tz**; third row: (G) brightfield, (H) overlay of blue and green channels, (I) overlay of brightfield, blue and green channels of cells treated with **1** and subsequently **OG-Tz** and Hoechst 33258; fourth row: (J) brightfield, (K) overlay of red and green channels, (L) overlay of brightfield, red and green channels of cells treated with **1** and subsequently **OG-Tz** and MitoTracker® Red CM-H2XRos; fifth row: (M) brightfield, (N) overlay of red and green channels, (O) overlay of brightfield, red and green channels of cells treated with **1** and subsequently **OG-Tz** and LysoTracker® Red DND-99.

(over 10-fold enhancement of signal-to-noise ratio relative to the MS/MS signal for total cellular RNA). These observations suggest that rRNA is the primary destination of the adenosine analogue.

Fluorescent labelling of ribosomal RNA inside of live mammalian cells was carried out using tetrazine conjugated to Oregon Green fluorophore, **OG-Tz**.[16] Devaraj and co-workers reported that **OG-Tz** is capable of producing a strong enhancement of fluorescence as the result of IEDDA reaction. Indeed, the reaction between **OG-Tz** and **1** resulted in a 28-fold fluorescence enhancement (Scheme 1C). Live HeLa cells were treated with **1** (100 μM) for 24 h. The concentration was chosen to be analogous to the previously reported protocols for **EU**.[7a] MTT assay, shown in Fig. S2 (ESI†), confirmed that **1** is not cytotoxic at the chosen concentration range. Subsequently, the cells were grown in fresh DMEM for 3 h and treated with the **OG-Tz** (5 μM) for 2 h.

The two-step bio-orthogonal chemistry approach resulted in fluorescent labelling of ribosomal RNA inside of live HeLa cells. The punctate staining observed in the cells treated with **1** and **OG-Tz** (Fig. 2D–F) has been attributed to rRNA. Cells treated with DMSO, as a negative control, and **OG-Tz** were weakly fluorescent (Fig. 2A–C). Unfortunately, there are no other imaging probes for rRNA that could be employed to verify that the observed staining is largely due to rRNA. We carried out colocolization studies with Hoechst 33258 (Fig. 2G–I), MitoTracker® Red CM-H2XRos (Fig. 2J–L) and LysoTracker® Red DND-99 (Fig. 2M–O) to confirm that the observed punctate staining is not associated with cellular DNA, mitochondria or endosomes. Fig. 2G–I illustrates that the green fluorescence is not associated with cellular nuclei, while Fig. 2J–L confirms that **OG** fluorescence is not associated with mitochondria. Partial colocolization with LysoTracker® Red DND-99 has been observed (Fig. 2M–O). We think that partial colocolization could be due to endosomal uptake of **OG-Tz**. Cell images at higher magnification confirm that the majority of green puncta

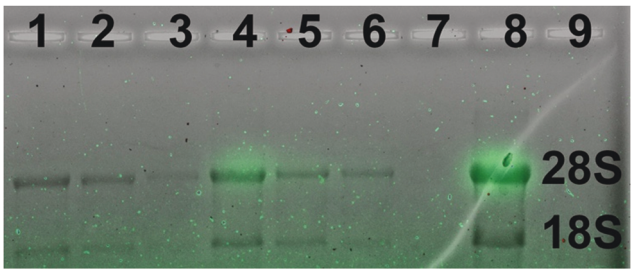

Fig. 3 Agarose gel (1%) analysis of total RNA extracted from HeLa cells. Shown is an overlay of the fluorescent image of the gel and staining with ethidium bromide. Lanes 1–3 correspond to total RNA extracted from the untreated HeLa cells (neg. control). The total amount of loaded RNA in each lane was 2 μg, 1 μg and 0.5 μg, respectively. Lanes 4–6, 8 correspond to total RNA extracted from the HeLa cells treated with **1**. The total amount of loaded RNA in each lane was 2 μg, 1 μg, 0.5 μg and 4 μg, respectively. After the extraction and prior to gel electrophoresis, the extracted RNA was treated with **OG-Tz** and purified by ethanol precipitation.

do not colocolize with the lysotracker dye (Fig. S3, ESI†). Pearson correlation coefficient was calculated to be 0.12.

To confirm fluorescent labelling of rRNA, we extracted total RNA from HeLa cells and analysed the extracts using 1% agarose gel electrophoresis, shown in Fig. 3. Lanes 1–3 correspond to the untreated cells (negative control), while lanes 4–6, 8 correspond to the cells treated with 100 μM **1** for 24 h. Prior to gel electrophoresis, the extracted total RNA from both sets of cells was treated with 5 μM **OG-Tz** for 2 h and purified by ethanol precipitation. Ethidium bromide staining of the gel produced two distinct bands corresponding to 28S and 18S subunits of rRNA. Only RNA of the HeLa cells treated with **1** showed fluorescence staining of the 28S subunit. To confirm this result we also performed higher loading of RNA in lane 8 and observed strong fluorescent staining.

In conclusion, we have described the first example of a nucleoside analogue modified with a bio-orthogonal TCO group that is capable of incorporating into ribosomal RNA. The incorporation was achieved using aryl phosphoramidate strategy to mask the 5′-phosphate group of the adenosine analogue. The incorporation has been proven by fluorescence microscopy, gel electrophoresis and a highly sensitive UHPLC-MS/MS analysis. Unlike the previously reported RNA imaging methods involving CuAAC chemistry, our approach can be implemented in live cells. Because of the fast reactivity between TCO and Tz, the fluorescence labelling step takes only 3 h. The presented findings produced a number of critical questions that will undoubtedly be addressed in subsequent studies. In particular, the selectivity of **1** towards 28S subunit of rRNA will be investigated. MS/MS analysis will be employed to determine the site of incorporation of the adenosine analogue. Our findings also motivate further investigation of the aryl phosphoramidate strategy towards modification of other nucleoside analogues containing yet unexplored bio-orthogonal groups.

Conflicts of interest

There are no conflicts to declare.

Notes and references

1 (*a*) W. A. Velema, A. M. Kietrys and E. T. Kool, *J. Am. Chem. Soc.*, 2018, **140**, 3491–3495; (*b*) A. Kadina, A. M. Kietrys and E. T. Kool, *Angew. Chem., Int. Ed.*, 2018, **57**, 3059–3063.
2 H. Y. Park, H. Lim, Y. J. Yoon, A. Follenzi, C. Nwokafor, M. Lopez-Jones, X. Meng and R. H. Singer, *Science*, 2014, **343**, 422–424.
3 (*a*) J. M. Baskin, J. A. Prescher, S. T. Laughlin, N. J. Agard, P. V. Chang, I. A. Miller, A. Lo, J. A. Codelli and C. R. Bertozzi, *Proc. Natl. Acad. Sci. U. S. A.*, 2007, **104**, 16793–16797; (*b*) J. M. Baskin, K. W. Dehnert, S. T. Laughlin, S. L. Amacher and C. R. Bertozzi, *Proc. Natl. Acad. Sci. U. S. A.*, 2010, **107**, 10360–10365.
4 (*a*) J. Yang, J. Seckute, C. M. Cole and N. K. Devaraj, *Angew. Chem., Int. Ed.*, 2012, **51**, 7476–7479; (*b*) T. W. Bumpus and J. M. Baskin, *ACS Cent. Sci.*, 2017, **3**, 1070–1077.
5 (*a*) D. S. Liu, A. Tangpeerachaikul, R. Selvaraj, M. T. Taylor, J. M. Fox and A. Y. Ting, *J. Am. Chem. Soc.*, 2012, **134**, 792–795; (*b*) K. Wang, A. Sachdeva, D. J. Cox, N. M. Wilf, K. Lang, S. Wallace, R. A. Mehl and J. W. Chin, *Nat. Chem.*, 2014, **6**, 393–403.
6 (*a*) H. D. Halicka, E. Bedner and Z. Darzynkiewicz, *Exp. Cell Res.*, 2000, **260**, 248–256; (*b*) J. K. Larsen, P. O. Jensen and J. Larsen, *Curr. Protoc. Cytom.*, 2001, ch. 7, unit 7.12, pp. 7.12.1–7.12.11.
7 (*a*) C. Y. Jao and A. Salic, *Proc. Natl. Acad. Sci. U. S. A.*, 2008, **105**, 15779–15784; (*b*) D. Qu, L. Zhou, W. Wang, Z. Wang, G. Wang, W. Chi and B. Zhang, *Anal. Biochem.*, 2013, **434**, 128–135; (*c*) D. Curanovic, M. Cohen, I. Singh, C. E. Slagle, C. S. Leslie and S. R. Jaffrey, *Nat. Chem. Biol.*, 2013, **9**, 671–673.
8 (*a*) A. Naik, J. Alzeer, T. Triemer, A. Bujalska and N. W. Luedtke, *Angew. Chem., Int. Ed.*, 2017, **56**, 10850–10853; (*b*) K. Schmid, M. Adobes-Vidal and M. Helm, *Bioconjugate Chem.*, 2017, **28**, 1123–1134.
9 P. N. Asare-Okai, E. Agustin, D. Fabris and M. Royzen, *Chem. Commun.*, 2014, **50**, 7844–7847.
10 (*a*) H. Wu, S. C. Alexander, S. Jin and N. K. Devaraj, *J. Am. Chem. Soc.*, 2016, **138**, 11429–11432; (*b*) J. Schoch, S. Ameta and A. Jäschke, *Chem. Commun.*, 2011, **47**, 12536–12537; (*c*) A. M. Pyka, C. Domnick, F. Braun and S. Kath-Schorr, *Bioconjugate Chem.*, 2014, **25**, 1438–1443.
11 M. L. Blackman, M. Royzen and J. M. Fox, *J. Am. Chem. Soc.*, 2008, **130**, 13518–13519.
12 Y. Zhang and R. E. Kleiner, *J. Am. Chem. Soc.*, 2019, **141**, 3347–3351.
13 (*a*) C. McGuigan, R. N. Pathirana, J. Balzarini and E. De Clercq, *J. Med. Chem.*, 1993, **36**, 1048–1052; (*b*) C. McGuigan, D. Cahard, H. M. Sheeka, E. De Clercq and J. Balzarini, *J. Med. Chem.*, 1996, **39**, 1748–1753; (*c*) A. Cho, L. Zhang, J. Xu, R. Lee, T. Butler, S. Metobo, V. Aktoudianakis, W. Lew, H. Ye, M. Clarke, E. Doerffler, D. Byun, T. Wang, D. Babusis, A. C. Carey, P. German, D. Sauer, W. Zhong, S. Rossi, M. Fenaux, J. G. McHutchison, J. Perry, J. Feng, A. S. Ray and C. U. Kim, *J. Med. Chem.*, 2014, **57**, 1812–1825.
14 M. Basanta-Sanchez, S. Temple, S. A. Ansari, A. D'Amico and P. F. Agris, *Nucleic Acids Res.*, 2016, **44**, e26.
15 G. Fuchs, A. N. Petrov, C. D. Marceau, L. M. Popov, J. Chen, S. E. O'Leary, R. Wang, J. E. Carette, P. Sarnow and J. D. Puglisi, *Proc. Natl. Acad. Sci. U. S. A.*, 2015, **112**, 319–325.
16 H. Wu, J. Yang, J. Seckute and N. K. Devaraj, *Angew. Chem., Int. Ed.*, 2014, **53**, 5805–5809.